



AENSI Journals

Australian Journal of Basic and Applied Sciences

ISSN:1991-8178

Journal home page: www.ajbasweb.com



## Path Generation of Sit to Stand Motion using Humanoid Robot

Bazli Bahar, Muhammad Fahmi Miskon, Norazhar Abu Bakar, Ahmad Zaki Shukor, Fariz Ali

Faculty of Electrical Engineering, Universiti Teknikal Malaysia Melaka, Melaka, Malaysia.

### ARTICLE INFO

#### Article history:

Received 25 December 2013

Received in revised form 22

February 2014

Accepted 26 February 2014

Available online 15 March 2014

#### Keywords:

STS, Alexander technique, multiple chair height, NAO robot.

### ABSTRACT

**Background:** The study of sit to stand motion (STS) gives high impact to the robotics field particularly in rehabilitation, exoskeleton, as well as humanoid robotics. Research in the STS field will promote the advancement of common humanoid motion hence make a robot more humanlike. With the capability of STS motion, the robot can be set at sitting position as a default home position and can be used for the purpose of long period application such as security and domestic robot. The main challenge in STS is in addressing the lift-off from chair. In solving the problem, two components involved in the humanoid STS motion system; (1) phase and trajectory planning and (2) motion control. These components should be designed so that the zero moment point (ZMP), centre of pressure (CoP), and centre of mass (CoM) must be in the support polygon.

**Objective:** This paper presents the development of Sit to Stand (STS) motion path generation method that can autonomously generate a stable STS path when standing from multiple chair height. The proposed system is designed to have two main phases. (1) CoM transferring that implements Alexander STS technique and (2) Stabilization Strategy that used IF-THEN rules as action selection and proportional controller as tracking method

**Results:** in the CoM transferring phase, NAO robot is able to shift the head-arms-torso system (HAT) CoM into the support polygon for chair height in between 90.45% to 115.45% from the shank length with the CoM transferring period,  $T_1$  between 0.25 to 1.0 second. With the present of the second phase, the result shows that the robot is able to perform a complete standing motion autonomously when chair height in between 90.45% to 147.73% from the shank length with constant value of  $T_1$ .

**Conclusion:** proposed method is able to control the robot in performing STS motion within 3.2 seconds and the lowest RMSE is 4.0021°. Combination of IF-THEN rules and proportional direction and speed controller help to minimize the sensor error and capabilities in making a proper action have increased. The method predicts to works well if the chair height is higher than 147.73% from the shank length based from the performance evaluation.

© 2014 AENSI Publisher All rights reserved.

**To Cite This Article:** Bazli Bahar, Muhammad Fahmi Miskon, Norazhar Abu Bakar, Ahmad Zaki Shukor, Fariz Ali., Path Generation of Sit to Stand Motion using Humanoid Robot. *Aust. J. Basic & Appl. Sci.*, 8(2): 168-182, 2014

## INTRODUCTION

The study of sit to stand motion (STS) gives high impact to the robotics field particularly in rehabilitation (Chuy *et al.*, 2006), exoskeleton (Strausser and Kazerooni, 2011) as well as humanoid robotics. Research in the STS field will promote the advancement of common humanoid motion hence make a robot more humanlike. With the capability of STS motion, the robot can be set at sitting position as a default home position and can be used for the purpose of long period application such as security and domestic robot. STS capability can also be implemented to other similar system such as exoskeleton robot, orthosis robot and FES system. In humanoid robotics field, the STS study has not been given emphasis until year 2010 (Mistry *et al.*, 2010). As far as 2013, groups have been identified to publish study of STS on humanoid are. M. Mistry, *et al.* (Mistry *et al.*, 2010), K. Qi, *et al.* (Kaicheng *et al.*, 2009), S. Pchelkin, *et al.* (Pchelkin *et al.*, 2010), M. Sakai *et al.* (Sakai *et al.*, 2010), G. Xue and H. Ballard (Xue and Ballard, 2006), J. Jones (Jones, 2011), P. Faloutsos, *et al.* (Faloutsos *et al.*, 2003), K. Kuwayama, *et al.* (Kuwayama *et al.*, 2003), S. Iida, *et al.* (Iida *et al.*, 2004), and M. Sugisaka (Sugisaka, 2007).

The main challenge in STS is addressing the lift-off from chair. The lift-off problem occurs when support polygon's area becomes smaller (initially positioned where hip touches the chair and feet touches the ground but becomes smaller when only the feet touches the ground) in a short period (Mistry *et al.*, 2010, Riley *et al.*, 1995). The phenomena is proven clinically in (Millington, 1992) where the result showed that many parameters including torque at each joint and position of CoM need to be controlled at this point within a short period (9%

**Corresponding Author:** Muhammad Fahmi Miskon, Mechatronics department, Faculty of Electrical Engineering, Universiti Teknikal Malaysia Melaka, Hang Tuah Jaya, 76100 Durian Tunggal, Melaka, Malaysia.

Ph: +606-5552304

E-mail (fahmimiskon@utem.edu.my).

of STS cycle). Failure to overcome this problem will cause the humanoid robot to fall on its back. This phenomena is called sitback failures in (Riley *et al.*, 1995). The lift-off problem is also caused by the actuator at the ankle that is not able to rotate the whole body in balancing the STS motion (Pchelkin *et al.*, 2010).

In solving the problem, the main components of the humanoid STS system are the (1) phase and trajectory planning and (2) motion control (Mistry *et al.*, 2010). These components should be designed so that the zero moment point (ZMP), centre of pressure (CoP), and centre of mass (CoM) stay in the support polygon. Combination of a proper phase, the right controller, and trajectory planning will solve lift-off problem.

For the first component, improper phase and trajectory planning will cause the robot joints to be in awkward positions. For example, at sitting position, if a robot bends forward too much, its ankle joint will be unable to provide enough force to balance the STS motion (Pchelkin *et al.*, 2010). There are several phase that have been introduced to plan a proper trajectory in STS motion. Stability strategy and momentum-transfer are used by O. Riley *et al.* (Riley *et al.*, 1991). Knee strategy and the trunk-hip strategy (Coghlin, 1994) and initial forward trunk lean and upward extension (Aissaoui and Dansereau, 1999) are another names that have been called to represent the motion. There is also a researcher who divide the motion into more than 2 phases such as the initiation phase, seat unloading and lift phase (Millington, 1992). L. Saint-Bauzel, *et al.* (Saint-Bauzel *et al.*, 2009) divide the motion to pre-acceleration, acceleration, start rising and rising phase. Other than identifying the need of the motion and separating them into phases, W. Fu-Cheng, *et al.* in (Fu-Cheng *et al.*, 2007) chooses to implement an Alexander STS technique (AT) into the robot motion by planning the CoM position during STS movement. Human demonstration is another method used in (Mistry *et al.*, 2010, Mettin *et al.*, 2007, Kaicheng *et al.*, 2009) to obtain the CoM and joint trajectory to perform stable human-like STS motion.

Within the humanoid research group, the phase was defined into two, generally called stability strategy and momentum-transfer (Riley *et al.*, 1990). Knee strategy and the trunk-hip strategy are other name that have been called to represent the motion (Coghlin, 1994). W. Fu-Cheng, *et al.* (Fu-Cheng *et al.*, 2007) chooses the Alexander technique to move the robot in ADAM models. There is also research that uses vision system to model the phase and trajectory using human motion as reference (Cole *et al.*, 2007, Mistry *et al.*, 2010).

Alexander technique is a method on how to use the whole body in daily activities (Macdonald, 1989). One of activity that is stressed by this technique is performing a STS motion. In STS motion, the technique creates a balance standing motion and all joint share the task (Goddard, 2003). The technique was proven to solve back pain problem (Paul Little, December 2008, Cacciatore *et al.*, 2005), and increase the stability of elderly standing motion (Dennis, 1999). In the robotic field, (Fu-Cheng *et al.*, 2007) was the only article identified to be applying this technique in performing STS motion using simulation environment called ADAM models. Generally, it can be seen that AT also divide the motion into two main phases where; (1) proper positioning of CoM before lift off. (2) extension of whole body while all joint move in simultaneously.

The second component i.e. motion control concerns on how well a humanoid robot follows the planned trajectory. The challenge is to control the whole body to manage how and when the system should react (Prinz *et al.*, 2007). A good control method also helps to solve the phase planning problem as mention in (Konstantin Kondak, 2003). There are two aspects that need to be considered in STS motion control that is (1) action selection and (2) tracking the planned trajectory. Action selection concerns on selecting the appropriate action to be taken in different robot condition. Tracking the planned trajectory concerns on ensuring accuracy of robot motion in joint or cartesian space.

#### **Action selection:**

Selection of appropriate action has been performed in the work of others using several methods. The function of action selection is to choose the proper effort at certain condition such as different phase, robot position, or time interval. One of the method proposed is using a MOSIAC as a feed forward controller where this system function as soft selector to activated certain modules (Andani *et al.*, 2007). In (Prinz *et al.*, 2007), the action selection is determined by the controller called by the author as high-level controller where generally responsible for whole STS motion. This controller will carefully switch between the controllers in the specific subtask. This effort is also made in (Rasool *et al.*, 2010) where fuzzy If-Then rules is applied as appropriate activation system to active any controllers in the local model. The work is also same in (Mughal and Iqbal, 2006a) and (Mughal and Iqbal, 2006b) where the fuzzy If-Then rules is implemented.

The main problem when designing a fuzzy system is in determining the appropriate fuzzy parameter. Common approach is by determining the parameter heuristically. However, heuristic method requires expert knowledge and the solution is local to robot configuration and environment. For this reason, this paper presents the implementation of IF-THEN rule using COP position for selecting appropriate action. This approach is not considered before by others since they used simulated environment where the real COP data is lacking. Since in this project hardware experimentation is involved, the COP data can be acquired naturally by using force sensitive resistor embedded in the robot's feet.

### Tracking the planned trajectory:

Some of the available approaches in tracking is described and combined together with action selection method. The optimal  $H_2$  controller is combined with fuzzy in (Mughal and Iqbal, 2006a) and (Mughal and Iqbal, 2006b) where the  $H_2$  controller act as tracking scheme and the fuzzy as action selection. In (Prinz *et al.*, 2007), the fuzzy controller is used to track the torque required at certain joint. The PID controller is also used in (Andani *et al.*, 2007) to track the desired trajectory. In (Konstantin Kondak, 2003) the system uses two control stages, (1) PD or PID controller with the output torque from it undergoes a second stage of (2) Non-linear controller. Another tracking approach is a combination of same type of controller,  $H_2$  and  $H_\infty$  optimal controller in (Mughal and Iqbal, 2008).

The tracking scheme can be develop by single controller or combination of multiple controllers in order to ensure the actual motion is mostly the same with the planned trajectory. Once again, fuzzy controller is one of the most used controllers and another controller that has been used by many is optimal controller.

### Summary of contribution:

There are two new contributions presented in this paper. Firstly, a new trajectory generation method that can autonomously generate a stable sit to stand path when standing from multiple chair height is proposed. Secondly, this was the first known attempt to investigate STS performance using hardware experimentation and implementation of Alexander STS technique in trajectory design.

## MATERIALS AND METHODS

Fig. 1 shows the system overview of the proposed sit to stand motion. The system is designed to have two main phases. (1) CoM transferring and (2) Stabilization Strategy. In the CoM transferring phase, the trajectory of the robot motion is planned based on Alexander STS technique. The Alexander technique focus on decreasing the force needed to perform the STS motion. Alexander techniques suggest that the legs should hip-width apart and feet are flat with the ground and not so far forward (Mac Donnell, 2000). In this research, the focus is to use hip, knee, and ankle joint to perform the task. Hip joint bending to front and ankle joint change is made to bring the head-arms-torso system (HAT) CoM into the support polygon.

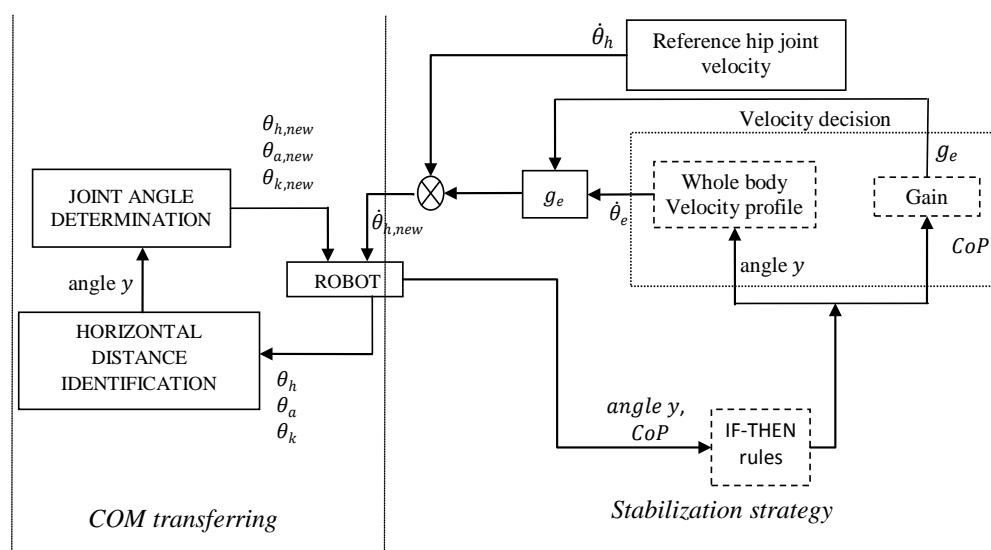


**Fig. 1:** Overall system overview for stable sit to stand motion.

Phase 2 starts when the HAT CoM is fully transferred in phase 1. In phase 2, the system will control the robot motion to a full standing position using velocity control. To determine a suitable velocity parameter value, IF-THEN rules are set. The rules is a decision controller that function in making a decision on velocity gain and direction. The gain is varied by the centre of pressure (CoP) position in x-axis. The position will vary for different humanoid robot.

### NAO robot configuration:

In this work, NAO robot has been used for experimentation purposes. NAO has three types of sensor to control its motion which is gyroscope, accelerometer, and force sensitive resistor. The gyrometer and

accelerometer is used to get the angle  $\gamma$  reading which refer to the angle between the robot and perpendicular line from the ground as in Fig. 2. Four units of FSR at the robot's feet give a CoP reading in meter.

The NAO robot version 3 came with two types of inertial unit, gyrometer with 5% precision and accelerometer 1% precision. Both sensors are located at the centre of the robot body. Four units of force sensitive resistors are located at each foot. All 6 motors at each controlled joint in this research are the same type with 8300rpm no load speed. However, results from a test shows that the motor speed is between 210 to 230 *degree/s* with load. All of the motor for one leg (3 unit motor) are align to each others.

#### System configuration:

The proposed method has two variables that need to be set before it can be implemented which are (1) CoM position and (2) CoP region boundaries.

#### CoM position:

The position of CoM between the CoM transferring phase and stabilization strategies phase are the same. This is because in the CoM transferring phase robot is at sit position. At this position thigh is support by the chair which brings that thigh and shank mass is neglected to plan the standing motion. The link that consider can affect the stability at this point is the robot body i.e head-arm-torso system (HAT). The CoM of HAT system is at 15.00cm from the hip joint.

In the second phase, The CoM is the same as before i.e HAT CoM. The assumption is based on the motion of thigh and shank link that move towards each other's and the mass of thigh and shank are mostly the same where  $m_t = 0.39421kg$ ,  $m_s = 0.29159kg$ . Mass that contributes most in the motion stability is the HAT CoM where it has a larger value,  $m_{HAT} = 3.02543kg$  and a higher position from the thigh and shank link.

#### Region boundaries:

The boundary is set using an experiment. The experiment was conduct using NAO robot that will perform the motion until the end of CoM transferring phase.

From the results, the most accepted value is from 0.03m to 0.025m. When  $x_{sr} = 0.02m$ , the robot fell to its front. The NAO robot is most stable when  $x_{sr} = 0.035m$  but the substantial distance between the HAT CoM and ankle joint will cause the robot to not perform well when faced with multi chair height. In this work,  $x_{sr}$  was set at 0.03m as the edge.

The the region for the IF-THEN rules, region back (*B*) is  $CoP < -0.02m$ , region middle (*M*) is  $-0.02m < CoP < 0.02m$ , and region front (*F*) is  $CoP > 0.02m$ . The 0.02m is used because region *M* represent as stable region where the edge should be larger than  $-0.03m$ . However, the region also cannot be too close to the ankle joint to avoid over sensitivity. The value 0.02m is also used as the front edge to represent the boundary between region *M* and *F*. The region position is described in Fig. 3.

#### CoM transferring phase:

The purpose of CoM transferring phase is to bring the HAT CoM into the support polygon that facilitate the stabilization strategy. In this phase, two processes were executed. (1) Horizontal distance,  $x_i$  identification, and (2) joint angle,  $\theta_h$  and  $\theta_a$  determination.

In the first process the horizontal distance between the HAT CoM of the robot with the ankle joint is identified. Next the change of angle at hip and ankle joint is determined. These parameter values are needed to bring the HAT CoM into the defined support polygon. In the first process, the horizontal distance  $x_i$  is determined by using (1).

$$\begin{aligned}
 x_i &= \pm[\alpha_h] + [\alpha_k] \pm [\alpha_a] & (1) \\
 \text{Where;} \quad \alpha_h &= \sin(|diff(\theta_{Rh}, \theta_{Nh})|) \times l_{CoM} \\
 \alpha_k &= \cos(|diff(\theta_{Rk}, \theta_{Nk})|) \times l_{thigh} \\
 \alpha_a &= \sin(|diff(\theta_{Ra}, \theta_{Na})|) \times l_{shank}
 \end{aligned}$$

The *diff* refers to difference between hip, knee and ankle joint position read from sensor,  $\theta_{Rh}, \theta_{Rk}, \theta_{Ra}$  with hip, knee and ankle joint position at normal position,  $\theta_{Nh}, \theta_{Nk}, \theta_{Na}$ .  $l_{CoM}$  is the length between hip joint to the HAT CoM in *cm* and  $l_{thigh}$  and  $l_{shank}$  is the length of thigh and shank. (1) is a x-axis component in the kinematic of the system. The equation represent in sensory unit so it can directly implement at any system. Fig. 2 shows the position of each joint and the normal position that has been defined.

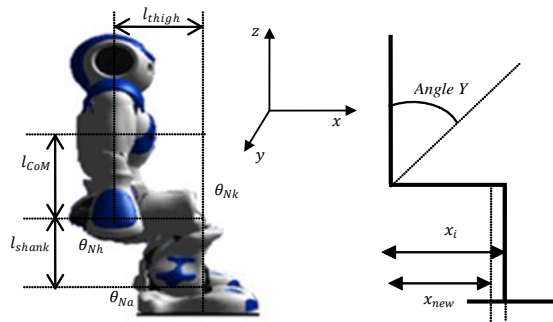


**Fig. 2:** The normal position of NAO robot at sitting position.

Typical parameter values for standard NAO sitting position use in this research is shown in Fig. 2:

$\theta_{Nh}$	=	-75.5 degree
$\theta_{Nk}$	=	90 degree
$\theta_{Na}$	=	-7 degree
$l_{COM}$	=	15 cm
$l_{thigh}$	=	10 cm
$l_{shank}$	=	10.3 cm

With (1), the distance of HAT CoM with ankle joint can be determine for any robot after normal sit position has been defined. hip joint unit,  $a_h$  can be ignored in (1), when the HAT CoM position is adjusted to be parallel with the hip joint position using (2).

$$\theta_{h.new} = \theta_{Nh} + [\theta_{Nk} - \theta_{Rk}] \quad (2)$$

In the second process, joint angle  $\theta_h$  and  $\theta_a$  is determined. Value  $x_i$  is used to identify angle change at each joint. The joint angle need to be identified to make sure that the HAT CoM is in the support polygon (SP). Referring to the Alexander technique, the method used the hip and ankle joint to shift upper body weight into the SP. In the first move, the method brings the body to the front. By using (3), the needed hip joint angle change  $\theta_{h.need}$  is calculated.

$$\theta_{h.need} = \theta_{Rh} - [90 - \text{abs}(\cos^{-1}(x_{new}/l_{COM}))] \quad (3)$$

Result from (3) is observed to make sure that the robot does not exceed the hip joint limitation. If the needed hip joint value,  $\theta_{h.need}$  is larger than the hip joint limit angle, the new hip joint angle is set to be equal to the maximum hip joint angle i.e.  $\theta_{h.new} = \theta_{h.max}$ . However, if  $\theta_{h.need}$  is smaller,  $\theta_{h.new} = \theta_{h.need}$ .  $x_{new}$  is the horizontal distance between the HAT CoM position with the edge of the SP. Ankle joint is another joint that will react if the HAT CoM still does not reached the SP edge. The limitation at hip joint leads to the needed of ankle joint change. At this point, remaining distance between HAT CoM and SP edge is calculated using (4).

$$x_{remain} = x_{new} - \text{abs}[(l_{COM} \times \cos(90 - (\theta_{Rh} - \theta_{h.new})))] \quad (4)$$

The remaining distance,  $x_{remain}$  determine whether the ankle joint change is needed or not. If  $x_{remain} = 0$ , the system proceed to the second phase. However, if  $x_{remain}$  has a positive value a new ankle joint is calculated using (5).

$$\theta_{a.new} = \theta_{Ra} + [-(\sin^{-1}(x_{remain}/l_{shank})) - \text{abs}(\theta_{Na} - \theta_{Ra})] \quad (5)$$

After both hip and ankle joint has their values, the system moves the robot to the desired position starting with hip than followed by ankle.

The trajectory of the hip and ankle joint is generated using the cubic polynomial function. With the cubic polynomial trajectory generation the joint speed was decreased at the first and the end of the motion. This condition directly affects the dynamic of the whole body motion. From time is 0 until first phase end,  $t_1$  the motion of hip, knee and ankle joint as in (6).

$$\theta = a_0 + a_1 t + a_2 t^2 + a_3 t^3 \quad (6)$$

Where,

$$a_0 = \theta_{Rh,a,k}$$

$$a_1 = 0$$

$$a_2 = \frac{3}{t_1^2} (\theta_{Rh,k,a} - \theta_{h,k,anew})$$

$$a_3 = \frac{2}{t_1^3} (\theta_{Rh,k,a} - \theta_{h,k,anew})$$

$\theta_{Rh,k,a}$  represents the angle reading at the first moment of sit position for hip, knee, and ankle joint.  $\theta_{h,k,anew}$  is the destination of each joint based from the new angle given from the joint angle determination process. Hip and ankle joint will rotate to the new angle while knee joint is the same. The motion will start with hip joint motion first and ankle joint start to rotate after hip joint has already at the destination. In between this motion, system will always monitor the projected angle  $y$  reading to make sure the robot does not fall forward. Hip or ankle joint will stop moving when angle  $y$  reading is more than the limit variable to control the motion from giving to much forward force. The pseudo code of the process is as follows:

```

1 :  $x_i = [\alpha_k] \pm [\alpha_a]$ 
2 :  $x_{new} = x_i - x_e$ 
3 :  $\theta_{h,need} = \theta_{Rh} - [90 - \text{abs}(\cos^{-1}(x_{new}/l_{COM}))]$ 
4 :
5 : If  $\theta_{h,need} < \theta_{h,max}$ 
6 :  $\theta_{h,new} = \theta_{h,need}$ 
7 : Else
8 :  $\theta_{h,new} = \theta_{h,max}$ 
9 :
10 :  $x_{remain} = x_{new} - \text{abs}[(l_{COM} \times \cos(90 - (\theta_{Rh} - \theta_{h,partial})))]$ 
11 : If  $x_{remain} > 0$ 
12 :  $\theta_{a,new} = \theta_{Ra} + [-(\sin^{-1}(x_{remain}/l_{shank}))\text{abs}(\theta_{Na} - \theta_{Ra})]$ 
13 : Else
14 :  $\theta_{a,new} = \theta_{Ra}$ 
15 :
16 : If angle  $y < \text{limit } y$ 
17 : If  $\theta_h < \theta_{h,new}$ 
18 : hip joint rotate
19 : Else
20 : ankle joint rotate
21 : Else
22 : move to second phase

```

### Stabilization strategy:

In this phase, controller input is CoP, in meter, angle  $y$ ,  $\theta_y$  and joint angle,  $\theta_{Rh/Rk/Ra}$ . The controller output is the new hip joint target angle,  $\theta_{h,new}$  and joint speed,  $\dot{\theta}_{h,new}$ . Firstly, the controller undergoes IF-THEN rules to choose the correct direction, velocity and gain. The gain and rules is based on the CoP position in three types of regions as depicted in Fig. 3. The boundaries of the regions are the optimum SP edge value. In this research the value is obtain using experimentation as mention in System configuration.

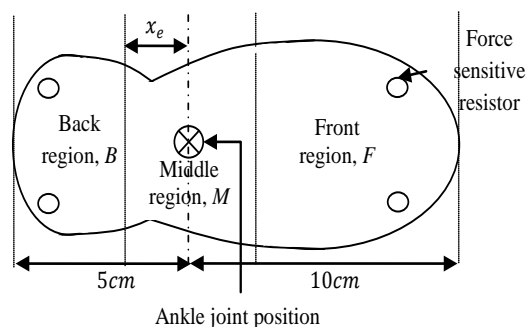


Fig. 3: Region defines at robot foot base on CoP position.

The robot is defined as stable when the CoP is in region  $M$  and becoming unstable when the CoP is in region  $B$  and  $F$  as shown in Fig. 3. The robot hip joint velocity,  $\dot{\theta}_{h.new}$  and direction,  $\theta_{h.new}$  depends on whether the CoP is in the region  $M$  or region  $B$  and  $F$  at the front or the back of the foot. Thus, the IF-THEN rules are set as follows:

IF: Angle  $y > \text{Plan}$  AND  $\text{CoP} > 0.02\text{cm}$

THEN: 1. Hip joint velocity is increased, 2. HAT moving backward direction, 3. Gain is based on region  $F$ .

IF: Angle  $y < \text{Plan}$  AND  $\text{CoP} < 0.02\text{cm}$

THEN: 1. Hip joint velocity is the body velocity error, 2. HAT moving forward direction, 3. Gain based on region  $B$ .

IF: Angle  $y > \text{Plan}$  AND  $(-0.02 < \text{CoP} < 0.02)$

THEN: 1. Hip joint velocity is increased, 2. HAT moving backward direction, 3. Gain based on region  $M$ .

IF: Angle  $y < \text{Plan}$  AND  $(-0.02 < \text{CoP} < 0.02)$

THEN: 1. Hip joint velocity is decreased, 2. HAT moving backward direction, 3. Gain based on region  $M$ .

#### Velocity decision:

The second output parameter from the controller is the velocity of the hip joint,  $\dot{\theta}_{h.new}$ . The velocity of hip joint is obtained from an inverted pendulum general formula. To do so, the HAT CoM position is assumed as the end point of an imaginary link that start from the ankle joint refer as whole body link as shown in Fig. 4. From now, the CoM of the whole robot was set located at the HAT CoM as the HAT give the most dynamic effect to the motion that state in (Hutchinson *et al.*, 1994) the HAT dynamic contribution is 10% to 15% and knee with ankle joint motion only less than 1%. Another link is the hip joint to the HAT CoM that becomes another system refers as body link.

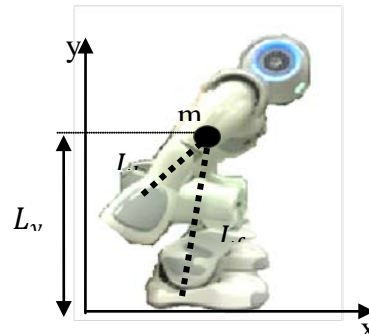


Fig. 4: Location of weight,  $m$  and the link of whole body link,  $L_f$  and body link,  $L_h$ .

The horizontal distance from ground to the centre of mass is,  $L_y$  obtained from the angle measurement. Using trigonometry concept, (7) is used to calculate the horizontal distance between ankle joint and the CoM.

$$L_y = Ych + Yck + Yca \quad (7)$$

Where,

$$Ych = |\cos(|diff(\theta_{Rh}, \theta_{Nh})|) \times l_{CoM}|$$

$$Yck = |\sin(|diff(\theta_{Rk}, \theta_{Nk})|) \times l_{thigh}|$$

$$Yca = |\cos(|diff(\theta_{Ra}, \theta_{Na})|) \times l_{shank}|$$

The link for whole body,  $L_f$  is determined by (8) and the link for body,  $L_h$  is always same as the distance between CoM and hip joint,  $l_{CoM}$ .

$$L_{fP} = \frac{L_y}{\cos \theta_{yP}}$$

$$L_{fR} = \frac{L_y}{\cos \theta_{yR}} \quad (8)$$

$\theta_{yP}$  and  $\theta_{yR}$  represent the plan and actual angle  $y$  trajectory. The general torque equation is,  $\tau_{net} = mgL \sin \theta$  that can also be represented by,  $\tau_{net} = mL^2 \ddot{\theta}$ . By combining both equations, it will be as in (9). The final formula for plan and actual value is used to calculate the error of angle  $y$  as in (10).

$$mL^2 \ddot{\theta} = mgL_f \sin \theta$$

$$\ddot{\theta} = \frac{g}{L_f} \sin \theta \quad (9)$$

$$\ddot{\theta}_e = \left[ \frac{g}{L_{fp}} \sin \theta_{yp} \right] - \left[ \frac{g}{L_{fR}} \sin \theta_{yR} \right] \quad (10)$$

From the acceleration error in (10), the velocity error is determined by integration of  $\ddot{\theta}_e$  within a step time. From the angular velocity error of the whole body motion, the tangential velocity,  $V_T$  error at CoM is determined using (11). A needed hip joint angular velocity is determined using (12). With the new angular velocity, a new tangential velocity  $V_{Tnew}$  that counter the first tangential velocity error generates by the whole body  $V_T$  was made by the upper body motion to ensure that the total  $V_{Tnet}$  error is zero.

$$V_T = \dot{\theta}_e \times L_{fR} \quad (11)$$

$$\dot{\theta}_{h,need} = \dot{\theta}_h \pm \frac{V_T}{L_{CoM}} \quad (12)$$

The new direction of the hip joint,  $\theta_{h,new}$  is determined base on angle y reading. From (10),  $\ddot{\theta}_e$  will be a positive or negative value depending on the value of  $\theta_{yR}$ . This in turn will influence the value of  $V_T$  and  $\dot{\theta}_{h,need}$  in (11) and (12).

#### Velocity gain:

The gain,  $g_e$  is determined from the CoP reading at the left feet. The value taken from only one foot because the system is analyze in 2 dimensions (X-Y) so position of CoP are mostly the same between each foot. At each region, the gradient,  $G$  was determined by experiment procedure using NAO robot. Both F and B regions are using the same gradient but M region has its own gradient. Gain for the controller after all motion is complete is determine in the same ways but different in gradient value. The gain,  $g_e$  is determined using (13). The new hip joint angular speed,  $\dot{\theta}_{h,new}$  is determine using (14).

$$g_e = G \times (CoP) \quad (13)$$

$$\dot{\theta}_{h,new} = \dot{\theta}_{h,need} \times K_e \quad (14)$$

## RESULTS AND DISCUSSION

This section discuss in detailed the results of three experiment conducted. Firstly, the experiment objective is to validate the proposed CoM transferring method and secondly, the stabilization strategy method, and the third is to validate the capability of the proposed method when facing a different chair's height. The experiment was done using NAO robot Version 3.3. Controller scheme was written using python script and no other external sensor was used. In every test, both robot's heels must touch the chair's front legs and the test was repeated for 5 times. Angle y and CoP position is observe to study the performance. Performance was measured by error happen in angle y trajectory calculated using root mean square error (RMSE).

#### CoM transferring:

Using a wooden chair, the height of chair was varied from 9.25 cm, 84.09% to 12.7 cm 115.45% from the shank length (SL). The shank length is 100% equivalent to 11.00cm where the shank is perpendicular with ground. To ensure the height is consistent, knee joint angle,  $\theta_k$  at initial was varied to represent the chair height; 90° is 11.0 cm or 84° is 12.05 cm. The STS motion was done until the end of CoM transferring phase where robot is at halfway from standing as in Fig. 4. This was made to ensure that the result was not influenced by the stabilization strategy phase. At first, hip joint and ankle joint change period is  $T_h = 0.25$  s and  $T_a = 0.25$  s. As the objective is to validate the capability of method proposed to transfer the HAT CoM into the stability edge,  $T_a$  was increased if the robot falls to its front. The result is shown in Fig. 5.

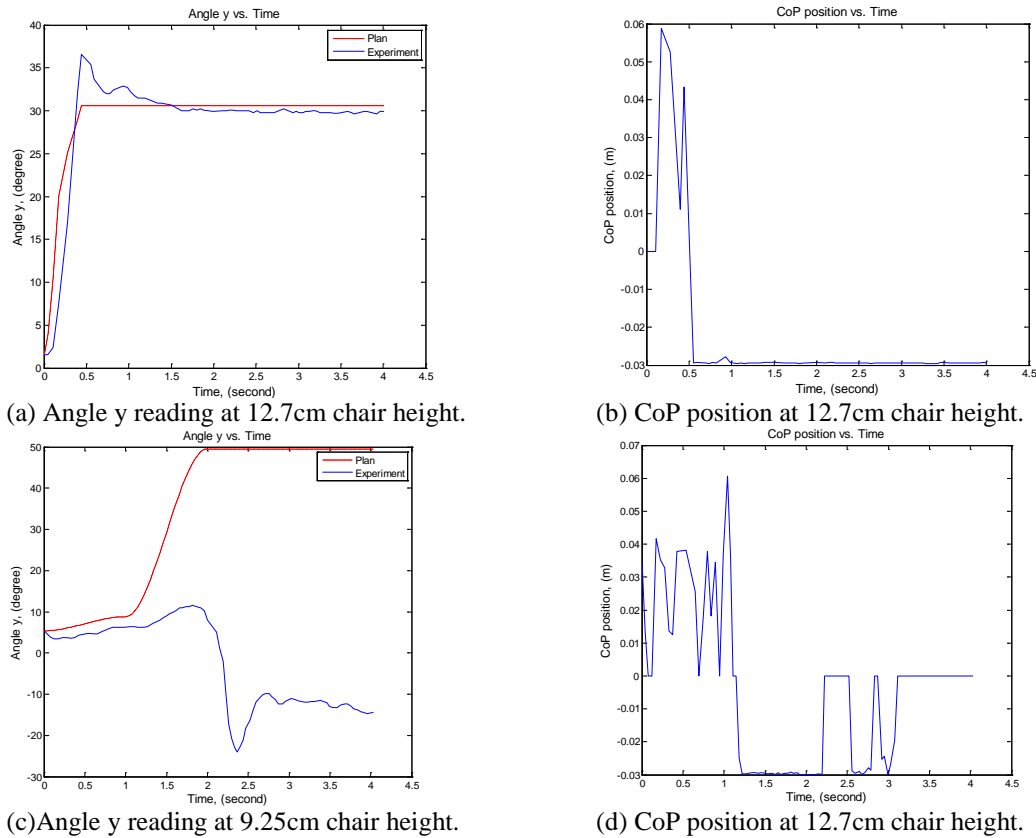


**Fig. 5:** The first graph (a) is the angle y trajectory when height of chair at 12.7cm and followed by (b) the CoP position. The third graph (c) is the result of angle y trajectory for chair height at 9.25cm and the last graph (d) is the CoP position at 9.25cm chair height.

Reading from four unit of Force Sensitive Resistor (FSR) at the left foot give the CoP at normal position is between 0.10m and -0.05m for the robot where it is at rest and stable. If the robot falls down, the reading is zero. The method was consider worked when the CoP is in the range of -0.03 to 0.01cm and angle y reading ended as straight line with  $\pm 5\%$  from the plan angle y.

With a new ankle joint,  $\theta_{a.new}$  and hip joint,  $\theta_{h.new}$  calculated by the method proposed, the robot was able to achieve the target position without falling within chairs height between 12.7 cm until 11.0 cm. After that, ankle joint change period,  $T_a$  was increased to ensure NAO achieve the target position as chair height decreasing. The relation between the ankle joint change period,  $T_a$  with the chair height as in Fig. 6.

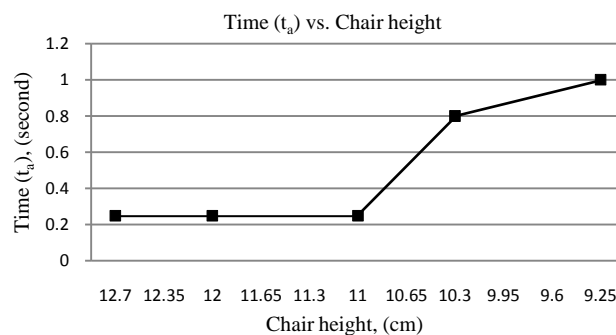


**Fig. 6:** Graph of ankle joint change time with chair height.

In the experimental result, chair height was varied to only 5 different values to optimize the robot usage. From the graph in Fig. 6, time needed for ankle joint change,  $T_a$  was increased at chair height 10.3 cm to ensure the robot would not fall to its front. This was due to the increasing of joint rotation when the chair height decreasing. Further discussion and the results is in (Mohd Bazli B. *et al.*, 2013).

**Stabilization strategy:**

In this experiment the chair height is set at 11cm where knee joint is at 90 degree. There is three gradient,  $G$  that identified and multi test method was used. The gradient that gives lower value of RMSE was chosen as the constant,  $G$ . The result this experiment is shown in Fig. 7. The gradient of each region is needed increase the flexibility of the proposed control method.

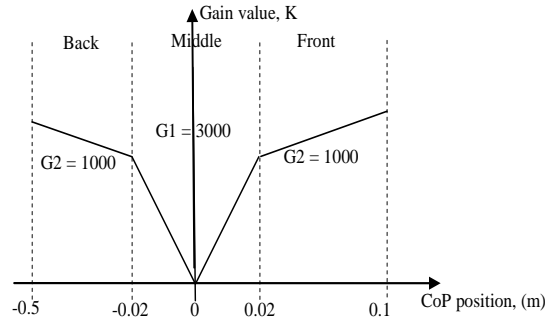


**Fig. 7:** The gain curve with the gradient and CoP.

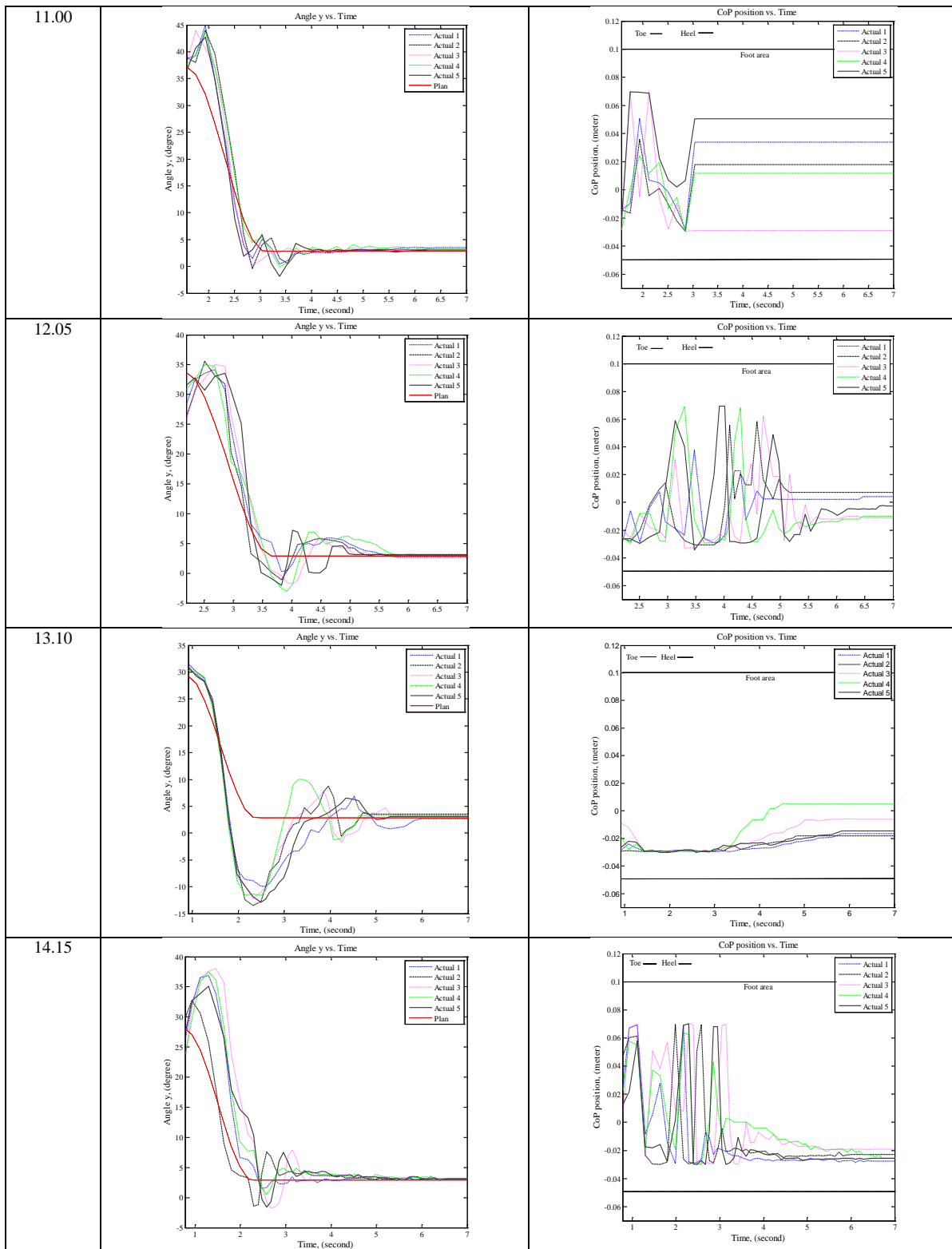
**Multi chair height:**

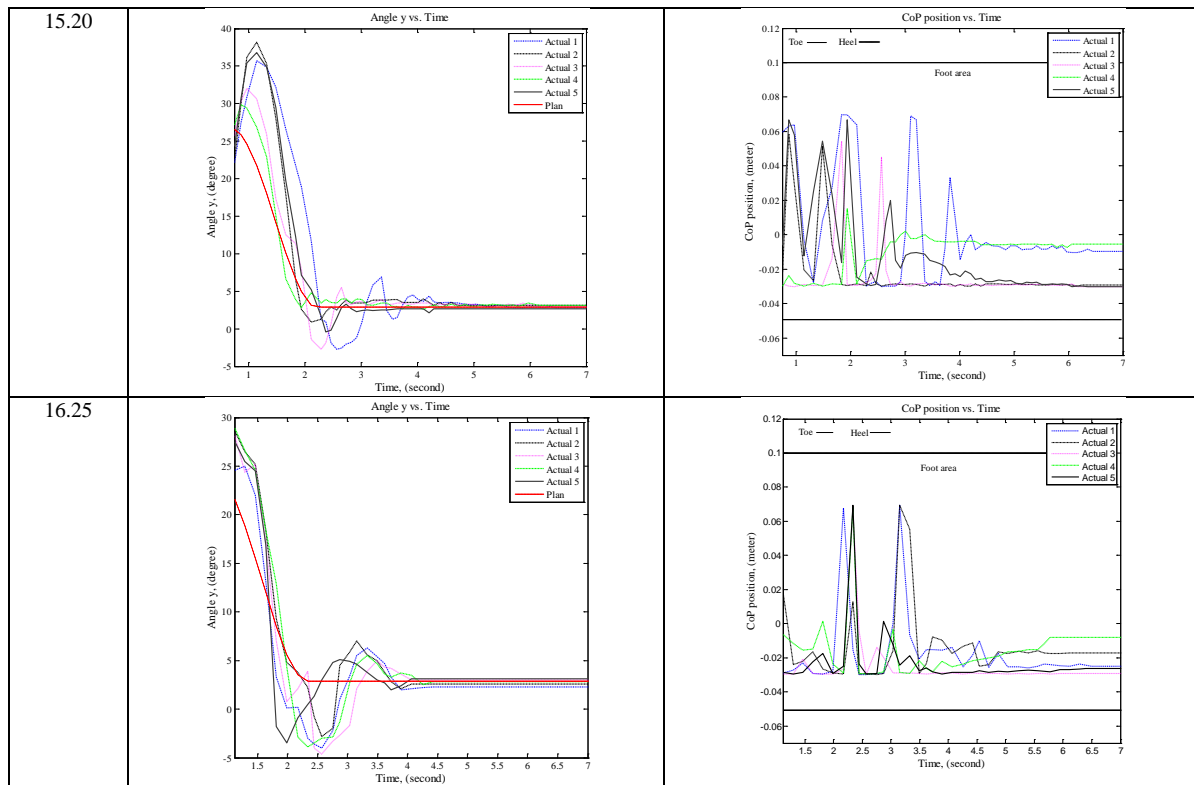
To validate the effectiveness of the proposed method, the complete system was tested with multiple chairs height. Using the same value of gradient in Fig. 7, the initial position of knee joint was changed to adapt the varied chair height. The knee joint value is adjusted  $6^\circ$  for each step. This is equivalent to 1.05cm increment of chair height. Thus, the chair height is 9.95, 11.0, 12.05, 13.10, 14.15, 15.20 and 16.25cm. The period set for CoM transferring phase,  $T_1$  is 2.0 second and the standing period,  $T_s$  is 1.5 second. The graph of angle  $y$  and CoP is shown start from the stabilization strategy until the end of the motion because the analysis of RMSE is done within this period. In the CoM transferring phase, the trajectory is the same as result in CoM transferring experiment.

From all the height tested, the robot was able to perform the motion completely except for chair height at 8.9cm. The angle  $y$  trajectory from 9.95cm to 16.25cm is similar but differ when chair height at 13.10cm. The results are shows in Table 1.

**Table 1:** Angle  $y$  and CoP position graph.

Chair height	Angle $y$	CoP position
9.95		





**Discussion:**

The CoP position when chair height is 8.9cm shows that the robot’s mass is focused at the back of the robot before moving instantly to zero where this represent that the robot’s feet does not touch the ground. When chair height is at 13.10cm, the CoP position does not changed much but still able to stand completely base from the final CoP position is not at zero and the angle y trajectory is approaching the plan trajectory. CoP position reading for others chair height is similar and the change is linear with the average RMSE of angle y trajectory. The average RMSE versus chair height graph is shown in Fig. 8.

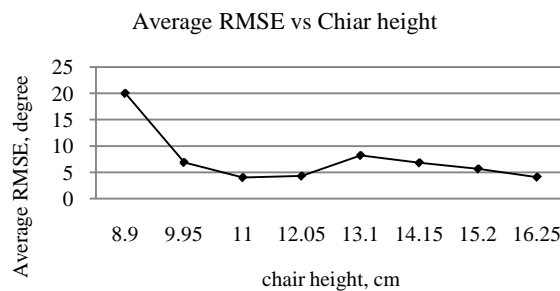


**Fig. 8:** Graph of average RMSE versus chair height.

The average RMSE is decreasing from 8.9cm to 11.00cm chair height than begin to increase back until 13.10cm. After that, the increasing of chair height will decrease the error happen in performing the task. The best performance is when chair height is at 11.00cm and the worst is 13.10cm exclude the falling that happen at 8.9cm.

From the result, robot fails to perform the task when chair height is at 8.9cm or 80.91% from the shank length (SL). This is because of HAT CoM is still located at the back of the robot. The angle y trajectory shows that the trajectory is less than 3° from the beginning of the standing motion. At this moment, hip joint is already at -87° to perform upright sitting position. So, only 2° is left for a hip joint to bend frontward due to the body limitation. The remaining horizontal distance for the ankle joint to react is 6.2565cm. When ankle joint begin to move, the robot HAT weight is still further at the back of the robot where it will experience a sitback.

Result when chair height is set at 13.10cm or 119.09% from SL is different from others because of involvement on ankle joint changes. As the ankle joint change start to decrease as the chair height increase, it will be no ankle change required when chair height more than 14.15cm. At 13.10cm, the ankle change only need to transfer the HAT CoM to another 0.2059cm where  $\theta_{a.new} = 8.1454^\circ$ . The change is only  $1.1454^\circ$  from the initial position. As the system will always monitor the angle  $\gamma$  trajectory so it not exceed to the front, motion of hip joint bending may already creates the momentum that reach this limitation. The effect is ankle joint change was never happen and the robot directly moves to the second phase i.e stabilization strategy.

For 13.10cm chair height, the position becomes the change point of performance refer to the average RMSE graph in Fig. 8. This is based on the involvement of ankle joint to transfer the HAT CoM into the SP. After 13.10cm, the ankle joint change is not needed as the chair height increase. The average RMSE begin to decrease when chair height increase because of hip joint change that decreasing as the robot initial position nearly to stand. The CoP position reading is also shown that the change from positive to negative position is decreasing. The decrease of hip joint change with constant change period,  $T_1 = 2 \text{ second}$  decrease the velocity of the hip joint motion thus generates less momentum to the front. The standing motion at this moment also becomes easier because change at each joint is decreasing. Once again, the overall velocity of the motion is decreased as the error at initial standing motion and motion velocity is lower when the chair height increases.

### Conclusion:

From the results, the proposed method is able to control the robot in performing STS motion within 3.2 seconds and the lowest RMSE is  $4.0021^\circ$ . The robot will collapse if there is no proper trajectory planning implement in the motion. AT that is proposed as a guideline in path planning able to transfer the HAT CoM into the define SP which helps to increase the stability of whole motion. Furthermore, the combination of IF-THEN rules and proportional direction and speed controller help to minimize the sensor error and capabilities to make proper action has increased. The proposed method is able to perform the STS motion at chair height 90.45% to 147.73% from the SL. The method predicts to works well if the chair height is higher than 147.73%. It is recommended for future work that the proposed method is tested on other biped robot to test the robustness and its capability. A new algorithm to find the best ankle joint change period,  $\Delta_\square$  by considers a various chair height condition will help to increase the robustness of the system. Furthermore, the STS dynamic model can also be diversified to identify the best model to be used in the system. In the future, the method and algorithm will be tested using others system such as exoskeleton to validate the CoM transferring phase for autonomous STS motion system.

### ACKNOWLEDGEMENT

The work was supported by Centre of Excellence, Robotics and Industrial Automation, Faculty of Electrical Engineering, Universiti Teknikal Malaysia Melaka and also sponsored by UTeM Study Leave Division and Malaysia Education Ministry (KPM).

### REFERENCES

- Aissaoui, R., J. Dansereau, 1999. Biomechanical analysis and modelling of sit to stand task: a literature review. *In: Systems, Man, and Cybernetics*,. IEEE SMC '99 Conference Proceedings. IEEE International Conference, 1: 141-146.
- Andani, M.E., F. Bahrami, P.J. Maralani, 2007. A Biologically Inspired Modular Structure to Control the Sit-to-Stand Transfer of a Biped Robot. *In: Engineering in Medicine and Biology Society, EMBS. 29th Annual International Conference of the IEEE*, 3016-3019.
- Cacciatore, T.W., F.B. Horak, S.M. Henry, 2005. Improvement in automatic postural coordination following Alexander technique lessons in a person with low back pain. *Physical therapy*, 85: 565-578.
- Chuy, O., Y. Hirata, W. Zhidong, K. Kosuge, 2006. Approach in Assisting a Sit-to-Stand Movement Using Robotic Walking Support System. *In: Intelligent Robots and Systems, IEEE/RSJ International Conference: 4343-4348*.
- Coghlin, S.S.M., 1994. Transfer strategies used to rise from a chair in normal and low back pain subjects. *In: Bioniech, Clin.*, 85-92.
- Cole, J.B., D.B. Grimes, R.P.N. Rao, 2007. Learning full-body motions from monocular vision: dynamic imitation in a humanoid robot. *In: Intelligent Robots and Systems, IROS 2007. IEEE/RSJ International Conference*, 240-246.
- Dennis, R.J., 1999. Functional reach improvement in normal older women after Alexander Technique instruction. *The Journals of Gerontology Series A: Biological Sciences and Medical Sciences*, 54: M8-M11.
- Faloutsos, P., M. Van De Panne, D. Terzopoulos, 2003. Autonomous reactive control for simulated humanoids. *In: Robotics and Automation, Proceedings. ICRA '03. IEEE International Conference*, 1: 917-924.

- Fu-Cheng, W., Y. Chung-Huang, L. Yi-Ling, T. Chen-En, 2007. Optimization of the Sit-to-Stand Motion. *In: Complex Medical Engineering. CME 2007. IEEE/ICME International Conference*, 1248-1253.
- Goddard, P., 2003. The Alexander Technique. Available: <http://www.clarity-of-being.org/alextech.htm#mozTocId797864> [Accessed 10.10.2013].
- Hutchinson, E.B., P.O. Riley, D.E. Krebs, 1994. A dynamic analysis of the joint forces and torques during rising from a chair. *Rehabilitation Engineering, IEEE Transactions on*, 2: 49-56.
- Iida, S., M. Kanoh, S. Kato, H. Itoh, 2004. Reinforcement learning for motion control of humanoid robots. *In: Intelligent Robots and Systems. (IROS 2004). Proceedings. 2004 IEEE/RSJ International Conference*, 4: 3153-3157.
- Jones, B.J., 2011. *Rising Motion Controllers for Physically Simulated Characters*. Master of Science, University Of British Columbia.
- Kaicheng, Q., G. Feng, L. Wei, Y. Jialun, 2009. Analysis of the state transition for a humanoid robot SJTU-HR1 from sitting to standing. *In: Mechatronics and Automation, ICMA 2009. International Conference*, 1922-1927.
- Konstantin Kondak, G.H., 2003. Control and Online Computation of Stable Movement for Biped Robots. *In: Ieee/Rsj (ed.) Intelligent Robots and Systems*. Las Vegas, Nevada: IEEE.
- Kuwayama, K., S. Kato, H. Seki, T. Yamakita, H. Itoh, 2003. Motion control for humanoid robots based on the concept learning. *In: Micromechatronics and Human Science, MHS 2003. Proceedings of 2003 International Symposium*, 259-263.
- Mac Donnell, M., 2000. *Alexander technique for health and well-being*, Southwater.
- Macdonald, P., 1989. *The Alexander Technique: As I See It*, Sussex Academic Press.
- Mettin, U., P. La Hera, L. Freidovich, A. Shiriaev, 2007. Generating human-like motions for an underactuated three-link robot based on the virtual constraints approach. *In: Decision and Control, 46th IEEE Conference*, 5138-5143.
- Millington, P.J., B.M. Myklebust, G.M. Shambes, 1992. Biomechanical Analysis of the Sit-to-Stand Motion in Elderly Persons. *Archives of Physical Medecine and Rehabilitation*, 73: 609-617.
- Mistry, M., A. Murai, K. Yamane, J. Hodgins, 2010. Sit-to-stand task on a humanoid robot from human demonstration. *In: Humanoid Robots (Humanoids), 2010 10th IEEE-RAS International Conference*, 218-223.
- Mohd Bazli, B., M.F. Miskon, A.B. Norazhar, S. Ahmad Zaki, A. Fariz 2013. Horizontal Distance Identification Algorithm for Sit to Stand Joint Angle Determination for Various Chair Height Using NAO Robot. *In: The 8th International Conference on Robotic, Vision, Signal Processing & Power Applications, H.A. Mat Sakim & M.T. Mustaffa, eds. 10-12 November 2013*.
- Mughal, A.M., K. Iqbal, 2006a. A Fuzzy Biomechanical Model for Optimal Control of Sit-to-Stand Movement. *In: Engineering of Intelligent Systems, 2006 IEEE International Conference*, 1-6.
- Mughal, A.M., K. Iqbal, 2006b. A Fuzzy Biomechanical Model with H2 Control System for Sit-to-Stand Movement. *In: American Control Conference*, 3427-3432.
- Mughal, A.M., K. Iqbal, 2008. Bipedal modeling and decoupled optimal control design of biomechanical sit-to-stand transfer. *In: Robotic and Sensors Environments, 2008. ROSE 2008. International Workshop*, 46-51.
- Paul Little, G.L., 2008. Fran Webley, Maggie Evans, Angela Beattie, Karen Middleton, Jane Barnett, Kathleen Ballard, Frances Oxford, Peter Smith, Lucy Yardley, Sandra Hollinghurst and Debbie Sharp. Randomised controlled trial of Alexander technique lessons, exercise, and massage (ATEAM) for chronic and recurrent back pain. *BMJ*.
- Pchelkin, S., A. Shiriaev, L. Freidovich, U. Mettin, S. Gusev, K. Woong, 2010. Natural sit-down and chair-rise motions for a humanoid robot. *In: Decision and Control (CDC), 2010 49th IEEE Conference*, 1136-1141.
- Prinz, R., S. Neville, N.J. Livingston, 2007. Development of a Fuzzy-Based Sit-to-Stand Controller. *In: Electrical and Computer Engineering, 2007. CCECE 2007. Canadian Conference*, 1631-1634.
- Rasool, G., A.M. Mughal, K. Iqbal, 2010. Fuzzy biomechanical sit-to-stand movement with physiological feedback latencies. *In: Systems Man and Cybernetics (SMC), 2010 IEEE International Conference*, 316-321.
- Riley, P.O., R. Popat, D.E. Krebs, 1995. Momentum analysis of sitback failures in sit-to-stand trials. *In: Engineering in Medicine and Biology Society, 1995., IEEE 17th Annual Conference*, 2: 1283-1284.
- Riley, P.O., M.L. Schenkman, R.W. Mann, W.A. Hodge, 1990. Comparison Of Paced And Unpaced Constrained Chair Rise Maneuvers. *In: Engineering in Medicine and Biology Society, Proceedings of the Twelfth Annual International Conference of the IEEE*, 2146-2147.
- Riley, P.O., M.L. Schenkman, R.W. Mann, W.A. Hodge, 1991. Mechanics of a constrained chair-rise. *Journal of Biomechanics*, 24: 77-85.
- Saint-Bauzel, L., V. Pasqui, I. Monteil, 2009. A Reactive Robotized Interface for Lower Limb Rehabilitation: Clinical Results. *Robotics, IEEE Transactions on*, 25: 583-592.
- Sakai, M., Y. Tomoto, M. Kanoh, T. Nakamura, H. Itoh, 2010. Acquisition of robot control rules by evolving MDDs. *In: Fuzzy Systems (FUZZ), 2010 IEEE International Conference*, 1-7.

Strausser, K.A., H. Kazerooni, 2011. The development and testing of a human machine interface for a mobile medical exoskeleton. *In: Intelligent Robots and Systems (IROS)*, 2011 IEEE/RSJ International Conference, 4911-4916.

Sugisaka, M., 2007. A control method for soft robots based on artificial muscles. *In: Mechatronics, ICM2007 4th IEEE International Conference*, 1-3.

Xue, G., D.H. Ballard, 2006. Motor Synergies for Coordinated Movements in Humanoids. *In: Intelligent Robots and Systems*, 2006 IEEE/RSJ International Conference, 3462-3467.